Detection of OH+ and H2O+ towards Orion KL

Astronomy & Astrophysics manuscript no. 15117arxiv
September 9, 2010

Detection of OH^+ and H_2O^+ towards Orion KL

H. Gupta,[1] P. Rimmer,[2] J. C. Pearson,[1] S. Yu,[1] E. Herbst,[2] N. Harada,[2] E. A. Bergin,[3] D. A. Neufeld,[4] G. J. Melnick,[5] R. Bachiller,[6] W. Baechtold,[7] T. A. Bell,[8] G. A. Blake,[8] E. Caux,[9,10] C. Ceccarelli,[11] J. Cernicharo,[12] G. Chattopadhyay,[1] C. Comito,[13] S. Cabrit,[14] N. R. Crockett,[3] F. Daniel,[12,15] E. Falgarone,[15] M. C. Diez-Gonzalez,[6] M.-L. Dubernet,[16,17] N. Erickson,[18] M. Emprechtinger,[8] P. Encrenaz,[15] M. Gerin,[15] J. J. Gill,[1] T. F. Giesen,[19] J. R. Goicoechea,[12] P. F. Goldsmith,[1] C. Joblin,[9,10] D. Johnstone,[21] W. D. Langer,[1] B. Larsson,[20] W. B. Latter[22] R. H. Lin,[1] D. C. Lis,[8] R. Liseau,[23] S. D. Lord,[22] F. W. Maiwald,[1] S. Maret,[11] P. G. Martin,[24] J. Martin-Pintado,[12] K. M. Menten,[13] P. Morris,[22] H. S. P. Müller,[19] J. A. Murphy,[25] L. H. Nordh,[20] M. Olberg,[23] V. Ossenkopf,[19,26] L. Pagani,[14] M. Pérault,[15] T. G. Phillips,[8] R. Plume,[27] S.-L. Qin,[19] M. Salez,[14] L. A. Samoska,[1] P. Schilke,[13,19] E. Schlecht,[1] S. Schlemmer,[19] R. Szczerba,[27] J. Stutzki,[19] N. Trappe,[25] F. F. S. van der Tak,[26] C. Vastel,[9,10] S. Wang,[3] H. W. Yorke,[1] J. Zmuidzinas,[8] A. Boogert,[8] R. Güsten,[17] P. Hartogh,[28] N. Honingh,[21] A. Karpov,[8] J. Kooi,[8] J.-M. Krieg,[12] R. Schieder[19] and P. Zaal[26]

(Affiliations can be found after the references)

Preprint online version: September 9, 2010

ABSTRACT

We report observations of the reactive molecular ions OH^+, H_2O^+, and H_3O^+ towards Orion KL with Herschel/HIFI. All three $N = 1 - 0$ fine-structure transitions of OH^+ at 909, 971, and 1033 GHz and both fine-structure components of the doublet *ortho*-H_2O^+ $1_{11} - 0_{00}$ transition at 1115 and 1139 GHz were detected; an upper limit was obtained for H_3O^+. OH^+ and H_2O^+ are observed purely in absorption, showing a narrow component at the source velocity of 9 km s^{-1}, and a broad blueshifted absorption similar to that reported recently for HF and *para*-$H_2^{18}O$, and attributed to the low velocity outflow of Orion KL. We estimate column densities of OH^+ and H_2O^+ for the 9 km s^{-1} component of $9\pm3\times10^{12}$ cm^{-2} and $7\pm2\times10^{12}$ cm^{-2}, and those in the outflow of $1.9\pm0.7\times10^{13}$ cm^{-2} and $1.0\pm0.3\times10^{13}$ cm^{-2}. Upper limits of 2.4×10^{12} cm^{-2} and 8.7×10^{12} cm^{-2} were derived for the column densities of *ortho* and *para*-H_3O^+ from transitions near 985 and 1657 GHz. The column densities of the three ions are up to an order of magnitude lower than those obtained from recent observations of W31C and W49N. The comparatively low column densities may be explained by a higher gas density despite the assumption of a very high ionization rate.

Key words. ISM: abundances — ISM: molecules

1. Introduction

The Heterodyne Instrument for Far Infrared (HIFI) on the *Herschel Space Observatory* [1] provides a unique opportunity to fully assess the first steps of the oxygen chemistry in a wide variety of sources. Initial HIFI observations quickly detected widespread absorption by OH^+ and H_2O^+ toward the star forming regions DR21, W31C, and W49N (Ossenkopf et al. 2010; Gerin et al. 2010; Neufeld et al. 2010, this issue). Prior to the HIFI observations, OH^+ had only been detected in absorption toward Sgr B2(M) (Wyrowski et al. 2010). Similarly, previous observations of H_2O^+ were limited to its detection in comet tails (e.g., Herzberg & Lew 1974; Wehinger et al. 1974), demonstrating the importance of photoionization in producing this ion in the absence of H_2. And until recently, only upper limits had been reported on the column density of H_2O^+ in the diffuse interstellar gas (Smith, Schempp, & Federman 1984).

By contrast, the recent HIFI detections of OH^+ and H_2O^+ in warm diffuse gas with a fairly small fraction of molecular hydrogen, elucidated the role of O^+ in initiating the oxygen-hydrogen chemistry. This chemistry is thought to begin with the production of H^+ and H_3^+ *via* cosmic ray or X-ray ionization of hydrogen, followed by charge transfer to produce O^+. Rapid hydrogen abstraction reactions of O^+ with H_2 then yield OH^+ and H_2O^+, and terminate with the production of H_3O^+. In diffuse molecular clouds, which have high electron abundances, the H_3O^+ is destroyed *via* dissociative recombination to yield OH and H_2O. In dense molecular clouds, both the ionization fraction and the atomic hydrogen abundance are comparatively lower, and the sequence of reactions, expected to start at H_3^+ and OH^+, yields a larger abundance of H_3O^+. This picture is probably overly simplistic for molecular clouds such as Orion KL, which are composed of both diffuse and dense gas.

Orion KL is the brightest infrared region in the Orion-Monoceros molecular cloud complex located less than 500 pc from the sun (Menten et al. 2007). In the foreground of Orion KL is the Orion Nebula, an HII region known to contain a cluster of thousands of young stars which produce a substantial flux of X-ray photons (Getman et al. 2005). Molecular line studies reveal three main regions in Orion KL: i. a core of very dense and hot gas ($n \sim 10^7$ cm^{-2}, $T \sim 200$ K); ii. cool, quiescent gas between systemic velocities of 8 km s^{-1} and 10 km s^{-1}, surrounded by high-velocity outflows ($\geq$ 100 km s^{-1}); and iii. a highly inhomogeneous and turbulent outflow source containing both high-velocity ($\geq$ 30 km s^{-1}) and low-velocity ($\sim$ 18 km s^{-1}) gas (Blake et al. 1987; Genzel & Stutzki 1989; O'Dell et al. 2008).

[1] *Herschel* is an ESA space observatory with science instruments provided by European-led Principal Investigator consortia and with important participation from NASA.

In this *Letter* we report the detection of absorption lines of OH^+ and H_2O^+, and an upper limit on the column density of H_3O^+ toward Orion KL. In addition to molecular absorption at a systemic velocity of 9 km s^{-1}, these observations find broad blueshifted absorption by OH^+ and H_2O^+ extending to large negative velocities. This is consistent with previously observed lines of H_2O with ISO (Lerate et al. 2006), as well as those of HF and *para*-$H_2^{18}O$ detected recently with HIFI, and attributed to the low-velocity molecular outflow (Phillips et al. 2010).

2. Observations and data reduction

The observations were done in March 2010 as part of the Key Program *Herschel/HIFI Observations of Extraordinary sources: The Orion and Sagittarius Star-forming Regions* (HEXOS). The dual beam switch (DBS) observing mode was used, with the DBS reference beams lying approximately 3′ east and west of the Orion KL position $\alpha_{J2000} = 5^h35^m14.3^s$ and $\delta_{J2000} = -5°22'33.7''$. Spectra were taken with the Wide Band Spectrometer (WBS) with a Nyquist-limited frequency resolution of approximately 1.1 MHz over a 4 GHz wide IF band; the HIFI beams in bands 4, 5, and 6 have half-power beam widths of 21″, 19″, and 13″ and main beam efficiencies of 0.670, 0.662, and 0.645 (HIFI Observers' Manual, v 2.0). The spectra were reduced through the standard Herschel Pipeline to Level 2 using HIPE version 2.4 (Ott 2010). The double sideband (DSB) spectra so obtained were then deconvolved (Comito & Schilke 2002) to single sideband (SSB) spectra using the *doDeconvolution* task in HIPE. The SSB spectra were converted to the FITS format and analyzed with the CLASS90 package. Although two orthogonal polarizations were observed simultaneously, only spectra from the H polarization in bands 4a and 6b and the V polarization in band 5a are shown, because of the smaller standing waves in these polarizations.

3. Spectroscopy

The spectroscopy of OH^+, H_2O^+, and H_3O^+ has been discussed in detail in the recent detection papers (Ossenkopf et al. 2010; Gerin et al. 2010). Here we summarize the essential aspects of the rotational spectra of these ions. The OH^+ ion has a $^3\Sigma^-$ electronic ground state, the two unpaired electron spins ($S = 1$) yielding three components of the $N = 1 - 0$ transition. The nuclear spin of the hydrogen atom ($I_H = 1/2$) further splits each component into hyperfine components. The H_2O^+ ion has C_{2v} symmetry and a $^2B_1$ ground state which results in the lowest level having *ortho* symmetry. The spin of the unpaired electron ($S = 1/2$) results in two fine-structure components, each exhibiting a complex hyperfine pattern due to the spins of the two equivalent hydrogen nuclei ($I_H = 1/2$). Rotational spectroscopy of H_2O^+ is limited to two laser magnetic resonance (LMR) studies (Strahan et al. 1986; Mürtz et al. 1998). Here, we adopt the values of Mürtz et al., which we and others have checked independently to be accurate to about 2 km s^{-1} in equivalent radial velocity (see Neufeld et al. 2010 and Schilke et al. 2010, this volume). H_3O^+ is a closed-shell symmetric top molecule with a large amplitude inversion near 1.65 THz, resulting in a spectrum similar to NH_3 with transitions between symmetric and antisymmetric inversion states (Yu et al. 2009). Table 1 lists the observed transitions of the three ions, along with their line strengths and spontaneous emission rates.

Table 1. Spectroscopic parameters of the observed transitions.

Transition	*Frequency*	E_l	g_l	g_u	$\mu^2 S$ [a]	$10^2 A_{ij}$
	(MHz)	(cm^{-1})			(D^2)	(s^{-1})
OH^+ $N = 1 - 0$ [b]						
$J = 1 - 0$						
$F = 1/2 - 1/2$	909045.2 ± 1.5	0.004	4	6	1.20	1.05
$1/2 - 3/2$	909158.8 ± 1.5	0	2	4	2.40	0.52
$J = 2 - 1$						
$F = 5/2 - 3/2$	971803.8 ± 1.5	0	4	6	10.24	1.82
$3/2 - 1/2$	971805.3 ± 1.5	0.004	2	4	5.69	1.52
$3/2 - 3/2$	971919.2 ± 1.0	0	4	4	1.14	0.30
o-H_2O^+ $1_{11} - 0_{00}$ [c]						
$J = 3/2 - 1/2$						
$F = 3/2 - 1/2$	1115150.0 ± 1.8	0.004	2	4	4.14	1.67
$1/2 - 1/2$	1115186.0 ± 1.8	0.004	2	2	3.32	2.68
$5/2 - 3/2$	1115204.0 ± 1.8	0	4	6	11.23	3.02
$3/2 - 3/2$	1115263.0 ± 1.8	0	4	4	3.35	1.35
$1/2 - 3/2$	1115298.7 ± 1.8	0	2	2	0.42	0.34
$J = 1/2 - 1/2$						
$F = 3/2 - 1/2$	1139541.1 ± 1.8	0.004	2	2	0.42	3.61
$1/2 - 1/2$	1139560.6 ± 1.8	0.004	2	4	3.35	1.44
$5/2 - 3/2$	1139653.5 ± 1.8	0	4	2	3.32	2.86
$3/2 - 3/2$	1139673.3 ± 1.8	0	4	4	4.14	1.78
H_3O^+ [d]						
$0_0^- - 1_0^+$	984711.9 ± 0.1[e]	5.1	4	12	8.30	2.30
$1_1^- - 1_1^+$	1655834.8 ± 0.3[f]	0	6	6	6.22	5.48
$2_2^- - 2_2^+$	1657248.4 ± 0.3[e]	29.6	10	10	4.67	7.32

Notes. [a] Dipole moments (μ): 2.256 D (OH^+; Werner, Rosmus, & Reinsch 1983); 2.37 D (H_2O^+; Wu et al. 2004); 1.44 D (H_3O^+; Botschwina, Rosmus, & Reinsch 1985). Frequencies from: [b] Müller et al. (2005); [c] Mürtz et al. (1998); [d] Yu et al. (2009)
[e] $\int T_A dv < 0.482$ K km s^{-1} for the 984.7 GHz line, and < 2.412 K km s^{-1} for the 1657.2 GHz line.
[f] Blended with a strong $2_{12} - 1_{10}$ *ortho*-$H_2^{18}O$ line at 1655831 MHz.

4. Results

Figure 1 shows the absorption lines of OH^+ and H_2O^+ toward Orion KL, as well as lines of HF and *para*-$H_2^{18}O$ for comparison. The strongest hyperfine components of OH^+ and H_2O^+ appear at the source velocity of 9 km s^{-1}, which matches well that of the HF line in Orion KL. Additionally, lines of both ions show broad blue absorption wings extending to about −75 km s^{-1}, more extended than the HF absorption, but comparable to that of *para*-$H_2^{18}O$ (~ -80 km s^{-1}). We attribute the extended absorption of the ions to originate mainly from the low velocity molecular outflow. We failed to detect any emission or absorption from H_3O^+, and discuss the non-detection in § 5.

The high density of molecular lines in Orion KL makes contamination by unrelated lines a common problem. The absorption lines detected here are blended with weak to moderately strong emission lines of abundant "weeds", including CH_3OH and SO_2. Efforts are underway to model and remove the emission from the contaminants by a method similar to that of Phillips et al. (2010); in the interim, the following approach was taken.

To better gauge the absorption, the contaminants were masked and intensities interpolated across the masked channels (Fig. 1). The velocity-integrated optical depths of the ionic lines were obtained by normalizing the SSB spectra with the continuum and integrating over the velocity ranges for the source

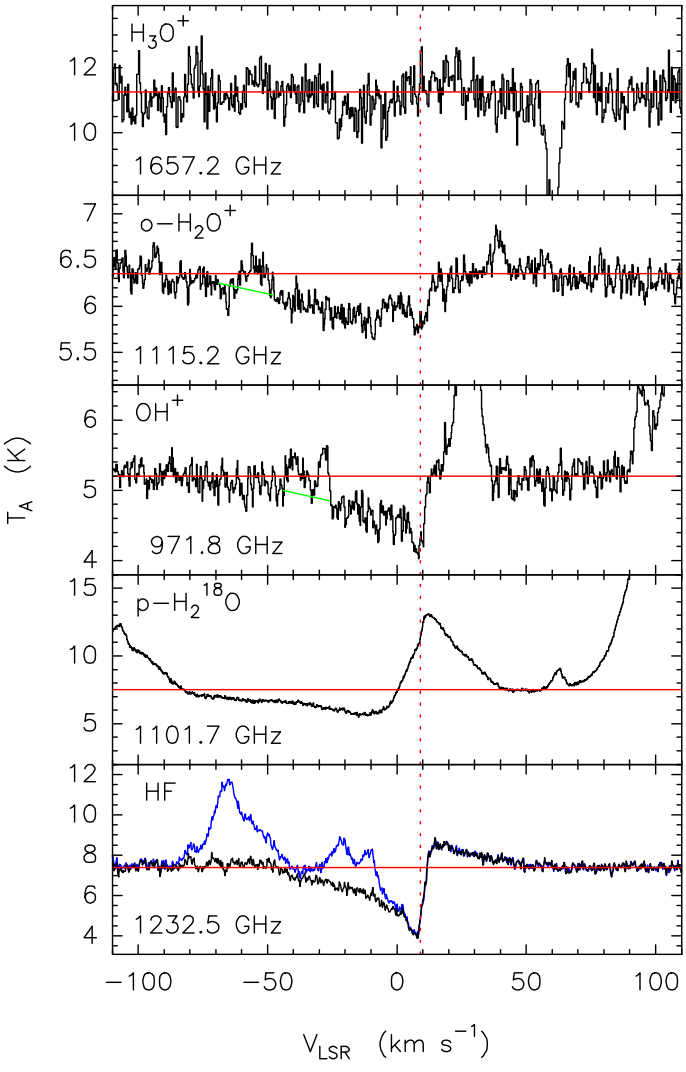

Fig. 1. Lines of OH^+, *ortho*-H_2O^+, and H_3O^+ in Orion KL, compared with those of HF ($J = 1 - 0$) and *para*-$H_2^{18}O$. The dashed vertical red line is at the systemic velocity of 9 km s^{-1}, and the solid horizontal red lines indicate the continuum level in each spectrum. Solid green lines indicate the channels over which the interpolation was done. The HF spectrum, adapted from Phillips et al (2010), shows a broad absorption (black histogram) after modeling and removal of contaminating lines of CH_3OH and SO_2 (blue histogram). The contaminants in the 971.8 GHz spectrum are CH_3OH ($v_t = 0$) $26_2^- - 25_3^-$ (A) and ($v_t = 1$) $22_6 - 22_5$ (E) at −28 km s^{-1} and −40 km s^{-1}; that in the 1115.2 GHz spectrum is SO_2 $19_{5,15} - 19_{2,18}$ at −55 km s^{-1}. The 1657.2 GHz spectrum shows absorption by CH ($N = 2 - 1$) at 60 km s^{-1}.

and the outflow, the interpolation yielding errors of 20% – 30%. On the assumptions that the absorption covers the source completely, and the molecules are in the lower state, the total column density (N) was then derived using the expression:

$$\int \tau dv \ (\mathrm{km\ s^{-1}}) = \frac{A_{ul} g_u \lambda^3}{8\pi g_l} N, \quad (1)$$

where A_{ul} is the spontaneous emission rate, g_u and g_l are the upper and lower state degeneracies, and λ is the transition wavelength.

We estimate column densities of OH^+ and H_2O^+ at 9 km s^{-1} of $9 \pm 3 \times 10^{12}$ cm^{-2} and $7 \pm 2 \times 10^{12}$ cm^{-2}, and those in the outflow of $1.9 \pm 0.7 \times 10^{13}$ cm^{-2} and $1.0 \pm 0.3 \times 10^{13}$ cm^{-2}. The column densities of OH^+ are more than an order of magnitude lower, and those of H_2O^+ are 2 – 6 times lower than toward W31C and W49N (Gerin et al. 2010; Neufeld et al. 2010, this issue). From the least congested spectra of H_3O^+ at 984.7 and 1657.2 GHz (see Table 1), and an assumed excitation temperature of 100 K, we derive 3σ upper limits of 2.4×10^{12} cm^{-2} and 8.7×10^{12} cm^{-2} for the column density of *ortho* and *para*-H_3O^+, nearly an order of magnitude lower than in W31C (Gerin et al. 2010).

The abundance ratios of the three ions in Orion KL can be compared to the same ratios observed in W31C and W49N. The OH^+/H_2O^+ ratio is found to be 1.3 ± 0.6 in the source and 1.8 ± 0.8 in the outflow. This ratio is 2 – 15 times lower than that measured toward W31C and W49N. The lower limit of 1.4 for the H_2O^+/H_3O^+ ratio, however, is nearly 2 times larger than in W31C.

5. Discussion

The column densities of OH^+, H_2O^+, and H_3O^+ in Orion KL differ markedly from those in the diffuse gas toward W31C and W49N. In contrast with W31C and W49N, OH^+ and H_2O^+ are significantly more abundant relative to H_3O^+, for which we are only able to obtain an upper limit. The absolute column densities of OH^+ and H_2O^+ are also lower compared with W31C and W49N. A likely explanation for the low column densities of the three ions is that they are present in fairly dense material, both in the quiescent gas and the outflow. Unlike the quiescent gas, the Orion KL outflow is exposed to a strong ionizing flux from the foreground HII region; the enhanced ionization flux enhances the formation of ions, but the resultant large fractional ionization leads to a fast and efficient removal of molecular ions by dissociative recombination with electrons.

The observed velocity profiles of OH^+ and H_2O^+ in Orion KL support the above conclusion. As Fig. 1 shows, the OH^+ and H_2O^+ absorption tracks the HF absorption to velocities of about −45 km s^{-1}. This absorption also seems to follow closely, to about −80 km s^{-1}, the *para*-$H_2^{18}O$ absorption in the outflow, suggesting that like HF and *para*-$H_2^{18}O$, OH^+ and H_2O^+ probably exist mainly in the low velocity outflow (Phillips et al. 2010). In fact, the molecular outflow accounts for over half of the observed column density of OH^+ and H_2O^+.

The conditions required to explain our observations may be more extreme than one might suppose. First, the molecular ions probably reside in gas of lower density ($n \leq 10^5$ cm^{-3}) than that necessary to thermally excite the observed transitions—these have high spontaneous emission rates ($> 10^{-2}$ s^{-1}; Table 1), and hence large critical densities ($10^7 - 10^9$ cm^{-3}) . This is supported by the observation that OH^+ and H_2O^+ are seen *only* in absorption. Second, the temperatures in the outflow gas are probably high.

We consider two scenarios in which the ions may be formed in the low velocity outflow. In the first, a large radiation flux impinges directly on the Orion KL outflow, which contains large water abundances (Melnick et al. 2010). The far UV flux that illuminates this gas can have values approaching 4×10^4 times the average interstellar radiation field (Walmsley et al. 2000; Young Owl et al. 2000). In addition, the central region of the Orion Nebula has numerous sources of energetic X-ray photons (Getman et al. 2005; Preibisch et al. 2005), which can contribute to the surface ionization of this photon-dominated region (PDR). We estimate that at $A_V = 1$ into the PDR, the ionization rate

$\zeta_X \sim 3 \times 10^{-15}$ s^{-1}. [2] Under these conditions, water can undergo photoionization to form H_2O^+ directly, enhancing the abundance of this species.

In the second scenario, the outflow penetrates the extended foreground HII region. The abundant H^+ can now undergo charge exchange with H_2O to yield H_2O^+. In either scenario, the high electron density probably results in a net reduction in the abundances of molecular ions, consistent with the observations: low column densities of OH^+ and H_2O^+, and the upper limit for H_3O^+.

We have attempted to model the first scenario using the Meudon PDR code (Le Petit et al. 2006). However, the model suffers difficulties while reproducing the observed column densities of the three ions. First, it requires a relatively low gas density ($n \sim 10^3$ cm^{-3}) in regions where OH^+ and H_2O^+ are produced, as larger assumed densities yield too much H_3O^+. Second, it requires a very large ionization rate ($\zeta > 1-2\times10^{-14}$ s^{-1}) to maintain a ratio of atomic to molecular hydrogen near unity; otherwise, too much H_3O^+ is once again produced. The two parameters are nearly an order of magnitude different from others inferred from previous observations: $n \geq 10^4$ cm^{-3} and $\zeta < 10^{-14}$ s^{-1} (Genzel & Stutzki 1989; Lerate et al. 2008; Muench et al. 2008 and references therein). Nevertheless, a recent study on molecular hydrogen rotational excitation in the Orion bar infers a cosmic ray ionization rate of 7×10^{-14} s^{-1} (Shaw et al. 2009). The same study also invokes warm gas temperatures of 400-700 K; the lower value is contained in our model for the edge of the PDR. A critical evaluation of our model awaits further work and a thorough exploration of the parameter space, and will be presented in a future paper.

We are unable to confirm previous tentative detections of H_3O^+ toward Orion KL (Hollis et al. 1986; Wootten et al. 1986; Wootten et al. 1991; Phillips et al. 1992; Timmermann et al. 1996; Lerate et al. 2006). Of these, Phillips et al. (1992) present the best evidence: 3 emission lines at 307, 364, and 396 GHz, lying 45, 85, and 105 cm^{-1} above ground; but they do not rule out the possibility of blends with other lines. The lines we observed are at lower energies (see Table 1), and are expected to be as strong or stronger than those observed by Phillips et al. (1992). The upper limits derived here for *ortho* and *para*-H_3O^+ are more than an order of magnitude lower than the column densities reported by Phillips et al. (1992). Timmermann et al. (1996) reported detection of the $4_3^- - 3_3^+$ line near 70 μm with the Kuiper Airborne Observatory, but the velocity of the line differs by more than -60 km s^{-1} from predicted values. Lerate et al. (2006) detected the $2_1^- - 1_1^+$, $2_0^- - 1_0^+$, and $1_1^- - 1_1^+$ lines with ISO: the first, near 2.98 THz is 80 km s^{-1} higher than the systemic velocity of 9 km s^{-1}; the second, near 2.97 THz, is 1 km s^{-1} higher than the frequencies predicted by Yu et al. (2009); and the third, at 1655835 MHz, covered by our observations, is obscured by a strong $2_{12} - 1_{10}$ *ortho*-$H_2^{18}O$ line at 1655831 MHz.

6. Conclusions

Our observations toward Orion KL have found OH^+ and H_2O^+ aborption at the quiescent 9 km s^{-1} component and extended absorption in the low velocity molecular outflow associated with this source. This is, to our knowledge, the first detection of these ions toward a source with a large fraction of molecular gas. Given the complex and inhomogeneous nature of Orion KL, however, there are probably regions where the densities are sufficiently low and the excitation conditions optimal for these reactive ions to exist at detectable levels. Another possibility is that depletion of some of the gas-phase species onto the grains can result in lower abundances of water, leading to small column densities of OH^+ and H_2O^+. A surprising observation—and one remarkably different from that toward W31C—is the non-detection of H_3O^+. In our model of the outflow, we attribute this mainly to a very high ionization rate, which produces an almost equal abundance of atomic and molecular hydrogen at the assumed density.

Acknowledgements. HIFI has been designed and built by a consortium of institutes and university departments from across Europe, Canada and the United States under the leadership of SRON Netherlands Institute for Space Research, Groningen, The Netherlands and with major contributions from Germany, France and the US. Consortium members are: Canada: CSA, U.Waterloo; France: CESR, LAB, LERMA, IRAM; Germany: KOSMA, MPIfR, MPS; Ireland, NUI Maynooth; Italy: ASI, IFSI-INAF, Osservatorio Astrofisico di Arcetri- INAF; Netherlands: SRON, TUD; Poland: CAMK, CBK; Spain: Observatorio Astronmico Nacional (IGN), Centro de Astrobiologa (CSIC-INTA). Sweden: Chalmers University of Technology - MC2, RSS & GARD; Onsala Space Observatory; Swedish National Space Board, Stockholm University - Stockholm Observatory; Switzerland: ETH Zurich, FHNW; USA: Caltech, JPL, NHSC. Support for this work was provided by NASA through an award issued by JPL/Caltech. A part of the work described in this paper was done at the Jet Propulsion Laboratory, California Institute of Technology, under contract with the National Aeronautics and Space Administration.

References

Blake, G. A., Sutton, E. C., Mason, C. R., & Phillips, T. G. 1987, ApJ, 315, 621
Botschwina, P, Rosmus, P., & Reinsch, E.-A. 1985, Chem. Phys. Lett., 102, 299
Comito, C., & Schilke, P. 2002, A&A, 395, 357
Feigelson, E. D., Getman, K. V., Townsley, L., et al. 2005, ApJS, 160, 379
Genzel, R., & Stutzki, J. 1989, ARA&A, 27, 41
Gerin, M., De Luca, M., Black, J. H., et al. 2010, A&A, arXiv:1005.5653
Getman, K. V., Feigelson, E. D., Grosso, M., et al. 2005, ApJS, 160, 353
Herzberg, G., & Lew, H. 1974, A&A, 31, 123
Lerate, M.R., Barlow, M.J., Swinyard, B.M., et al. 2006, MNRAS, 370, 597
Lerate, M.R., Yates, J., Viti, S., et al. 2008, MNRAS, 387, L1660
Le Petit, F., Nehmé, C., Le Bourtelot, J., & Roueff, E. 2006, ApJS, 164, 506
Maloney, P. R., Hollenbach, D. J., & Tielens, A. G. G. M. 1996, ApJ, 466, 561
Melnick, G. J., Tolls, V., Neufeld, D. A., et al. A&A, in press
Menten, K. M., Reid, M. J., Forbrich, J., & Brunthaler, A. 2007, A&A, 474, 515
Muench, A., Getman, K., Hillenbrand, L., & Preibisch, T. 2008 in ASP Monograph Publications 4, Handbook of Star Forming Regions, Vol. I: The Northern Sky ed. B Reipurth (San Francisco, CA: ASP), 483
Müller, H. S. P., Schlöder, F., Stutzki, J., & Winnewisser, G. 2005, J. Mol. Struct., 742, 215
Mürtz, P., Zink, L. R., Evenson, K. M., & Brown, J. M. 1998, J. Chem. Phys., 109, 9744
Neufeld, D. A., Goicoechea, J. R., Sonnentrucker, P., et al. 2010, arXiv:1007.0987
O'Dell, C. R., Muench, A., Smith, N., & Zapata, L. 2008 in ASP Monograph Publications 4, Handbook of Star Forming Regions, Vol. I: The Northern Sky ed. B Reipurth (San Francisco, CA: ASP), 544
Ossenkopf, V., Müller, H. S. P., Lis, D. C., et al. 2010, A&A, 518, L111
Ott, S. 2010, in ASP Conference Series, Astronomical Data Analysis Software and Systems XIX, Y. Mizumoto, K.-I. Morita, and M. Ohishi, eds., in press
Phillips, T. G., van Dishoeck, E. F., Keene, J. 1992 ApJ, 399, 533
Phillips, T. G., Bergin, E. A., Lis, D. C., et al. 2010, A&A, 518, L109
Preibisch, T., McCaughrean, M. J., Grosso, M., et al. 2005, ApJS, 160, 582
Schilke, P., Comito, C., Müller, H. S. P., et al. 2010, arXiv:1007.0670
Shaw, G., Ferland, G. J., Henney, W. J., et al. 2009 ApJS, 701, 677
Smith, W. H., Schempp, V. W., & Federman, S. R. 1984, ApJ, 277, 196
Strahan, S. E., Mueller, R. P., & Saykally, R. J. 1986, J. Chem. Phys., 85, 1252
Timmermann, R., Nikola, T., & Poglitsch, A. 1996, ApJ, 463, L109
Walmsley, C. M., Natta, A., Oliva, E. & Testi, L. 2000, A&A, 364, 301
Wehinger, P. A., Wyckoff, S., Herbig, G. H., Herzberg, G & Lew, H. 1974 ApJ, 190, L43

[2] The surface brightness of the central region (dominated by θ^1C) is estimated to be 3×10^{34} ergs s^{-1}pc^{-2} (Feigelson et al. 2005). On the assumption that the molecular cloud lies 0.1 pc from this cluster, the expressions of Maloney et al. (1996) yield an X-ray ionization rate of about $2.8 \times 10^{-16}N_{22}^{-1}$ (where N_{22} is the hydrogen column density in units of 10^{22} cm^{-2}). Thus at $A_V = 1$, $\zeta_X \sim 3 \times 10^{-15}$ s^{-1}.

Werner, H.-J, Rosmus, P., & Reinsch, E.-A. J. Chem. Phys., 1983, 79, 905
Wootten, A., Boulanger, F., Bogey, M. et al. 1986 A&A, 166, L15
Wootten, A., Mangum, J. G., Turner, B. E. et al. 1991, ApJ, 380, L79
Wu, S. Chen, Y. Yang, X., Guo, Y., Liu, Y., Li, Y., Buenker, R. J., & Jensen, P. 2004, J. Mol. Spec. 225, 96
Wyrowski, F., Menten, K. M., Guesten, R., & Belloche, A. 2010, arXiv:1004.2627
Young Owl, R. C., Meixner, M. M., Wolfire, M., Tielens, A. G. G. M. & Tauber, J. 2000, ApJ, 540, 886
Yu, S., Drouin, B. J., Pearson, J. C. & Pickett, H. M. 2009, ApJS, 180, 119

---

[1] Jet Propulsion Laboratory, Caltech, Pasadena, CA 91109, USA
e-mail: hgupta@jpl.nasa.gov
[2] Departments of Physics, Astronomy, and Chemistry, Ohio State University, Columbus, OH 43210, USA
[3] Department of Astronomy, University of Michigan, 500 Church Street, Ann Arbor, MI 48109, USA
[4] Department of Physics and Astronomy, Johns Hopkins University, 3400 North Charles Street, Baltimore, MD 21218, USA
[5] Harvard-Smithsonian Center for Astrophysics, 60 Garden Street, Cambridge MA 02138, USA
[6] Observatorio Astronómico Nacional (IGN), Centro Astronómico de Yebes, Apartado 148. 19080 Guadalajara, Spain
[7] Microwave Laboratory, ETH Zurich, 8092 Zurich, Switzerland
[8] California Institute of Technology, Cahill Center for Astronomy and Astrophysics 301-17, Pasadena, CA 91125 USA
[9] Centre d'étude Spatiale des Rayonnements, Université de Toulouse [UPS], 31062 Toulouse Cedex 9, France
[10] CNRS/INSU, UMR 5187, 9 avenue du Colonel Roche, 31028 Toulouse Cedex 4, France
[11] Laboratoire d'Astrophysique de l'Observatoire de Grenoble, BP 53, 38041 Grenoble, Cedex 9, France.
[12] Centro de Astrobiología (CSIC/INTA), Laboratiorio de Astrofísica Molecular, Ctra. de Torrejón a Ajalvir, km 4 28850, Torrejón de Ardoz, Madrid, Spain
[13] Max-Planck-Institut für Radioastronomie, Auf dem Hügel 69, 53121 Bonn, Germany
[14] LERMA & UMR8112 du CNRS, Observatoire de Paris, 61, Av. de l'Observatoire, 75014 Paris, France
[15] LERMA, CNRS UMR8112, Observatoire de Paris and École Normale Supérieure, 24 Rue Lhomond, 75231 Paris Cedex 05, France
[16] LPMAA, UMR7092, Université Pierre et Marie Curie, Paris, France
[17] LUTH, UMR8102, Observatoire de Paris, Meudon, France
[18] University of Massachusetts, Astronomy Dept., 710 N. Pleasant St., LGRT-619E, Amherst, MA 01003-9305 U.S.A
[19] I. Physikalisches Institut, Universität zu Köln, Zülpicher Str. 77, 50937 Köln, Germany
[20] Department of Astronomy, Stockholm University, SE-106 91 Stockholm, Sweden
[21] National Research Council Canada, Herzberg Institute of Astrophysics, 5071 West Saanich Road, Victoria, BC V9E 2E7, Canada
[22] Infrared Processing and Analysis Center, California Institute of Technology, MS 100-22, Pasadena, CA 91125
[23] Chalmers University of Technology, SE-412 96 Gteborg, Sweden, Sweden; Department of Astronomy, Stockholm University, SE-106 91 Stockholm, Sweden
[24] Canadian Institute for Theoretical Astrophysics, University of Toronto, 60 St George St, Toronto, ON M5S 3H8, Canada
[25] National University of Ireland. Maynooth, Ireland
[26] SRON Netherlands Institute for Space Research, PO Box 800, 9700 AV, Groningen, The Netherlands
[27] N. Copernicus Astronomical Center, Rabianska 8, 87-100, Torun, Poland
[28] Department of Physics and Astronomy, University of Calgary, 2500 University Drive NW, Calgary, AB T2N 1N4, Canada
[29] MPI für Sonnensystemforschung, D 37191 Katlenburg-Lindau, Germany